Received: 19 March 2020 | Revised: 12 April 2020 | Accepted: 17 April 2020

DOI: 10.1002/jmor.21135

RESEARCH ARTICLE

morphology WILEY

Armored with skin and bone: A combined histological and µCT-study of the exceptional integument of the Antsingy leaf chameleon *Brookesia perarmata* (Angel, 1933)

Pia J. Schucht[1] | Peter T. Rühr[2,3] | Benedikt Geier[4] | Frank Glaw[5] | Markus Lambertz[1,6]

[1]Institut für Zoologie, Rheinische Friedrich-Wilhelms-Universität Bonn, Poppelsdorfer Schloss, Bonn, Germany

[2]AG Morphologische Dynamiken, Institut für Zoologie, Biozentrum, Universität zu Köln, Köln, Germany

[3]Zentrum für Molekulare Biodiversitätsforschung, Zoologisches Forschungsmuseum Alexander Koenig, Bonn, Germany

[4]Max Planck Institute for Marine Microbiology, Bremen, Germany

[5]Sektion Herpetologie, Zoologische Staatssammlung München (ZSM-SNSB), Munich, Germany

[6]Sektion Herpetologie, Zoologisches Forschungsmuseum Alexander Koenig, Bonn, Germany

Correspondence
Markus Lambertz, Institut für Zoologie, Rheinische Friedrich-Wilhelms-Universität Bonn, Poppelsdorfer Schloss, 53115 Bonn, Germany.
Email: lambertz@uni-bonn.de

Peer Review
The peer review history for this article is available at https://publons.com/publon/10.1002/jmor.21135.

Abstract

Madagascar's endemic ground-dwelling leaf chameleons (Brookesiinae: *Brookesia* Gray, 1865 + *Palleon* Glaw, et al., Salamandra, 2013, 49, pp. 237–238) form the sister taxon to all other chameleons (i.e., the Chamaeleoninae). They possess a limited ability of color change, a rather dull coloration, and a nonprehensile tail assisting locomotion in the leaf litter on the forest floor. Most *Brookesia* species can readily be recognized by peculiar spiky dorsolateral projections ("*Rückensäge*"), which are caused by an aberrant vertebral structure and might function as body armor to prevent predation. In addition to a pronounced *Rückensäge*, the Antsingy leaf chameleon *Brookesia perarmata* (Angel, 1933) exhibits conspicuous, acuminate tubercle scales on the lateral flanks and extremities, thereby considerably enhancing the overall armored appearance. Such structures are exceptional within the Chamaeleonidae and despite an appreciable interest in the integument of chameleons in general, the morphology of these integumentary elements remains shrouded in mystery. Using various conventional and petrographic histological approaches combined with µCT-imaging, we reveal that the tubercle scales consist of osseous, multicusped cores that are embedded within the dermis. Based on this, they consequently can be interpreted as osteoderms, which to the best of our knowledge is the first record of such for the entire Chamaeleonidae and only the second one for the entire clade Iguania. The combination of certain aspects of tissue composition (especially the presence of large, interconnected, and marrow-filled cavities) together with the precise location within the dermis (being completely enveloped by the *stratum superficiale*), however, discriminate the osteoderms of *B. perarmata* from those known for all other lepidosaurs.

KEYWORDS
3D morphology, Brookesiinae, Chamaeleonidae, histology, integument, osteoderm

1 | INTRODUCTION

Chameleons as a whole (Squamata: Iguania: Chamaeleonidae) are captivating animals and their exceptional integument in general is morphologically well studied, especially with regard to color change (e.g., Best, 1968; Ligon & McGraw, 2013; Stuart-Fox & Moussalli, 2008; Teyssier, Saenko, Van Der Marel, & Milinkovitch, 2015; van der Hoeven, 1831) and microstructure (e.g., Canham, 1999; Riedel, Böhme, Bleckmann, & Spinner, 2015; Schleich & Kästle, 1985; Spinner, Westhoff, & Gorb, 2013). One of their more unusual clades is represented by the so-called leaf chameleons of the genus *Brookesia* Gray, 1865, which is endemic to Madagascar (Glaw, 2015) and which together with *Palleon* Glaw, Hawlitschek, & Ruthensteiner, 2013 forms the Brookesiinae, which in turn comprises the sister taxon to all remaining chameleons (Tolley, Townsend, & Vences, 2013; Townsend & Larson, 2002; Townsend, Vieites, Glaw, & Vences, 2009). These species are characterized by their more scansorial lifestyle in forest floor leaf litter than truly being arboreal and only retreat to low perches at night. Leaf chameleons are readily recognizable by a rather dull, mostly brownish coloration, a limited ability of color change, and a nonprehensile tail aiding as sort of additional limb during locomotion on the ground (Boistel et al., 2010). These rather inconspicuous chameleons include with *Brookesia micra* one of the world's smallest known amniote (Glaw, Köhler, Townsend, & Vences, 2012).

A striking morphological feature of this group concerns a more-or-less developed row of spiky projections running along their back. This *Brookesia*-specific "*Rückensäge*" ("spinal saw"; Boettger, 1878, 1893) and its underlying peculiar vertebral structure has been subject to several osteological studies, particularly in *Brookesia superciliaris* (Kuhl, 1820) (Parker & Taylor, 1942; Siebenrock, 1893). One of the larger species of the genus, the Antsingy leaf chameleon *Brookesia perarmata* (Angel, 1933), does not only exhibit a well-pronounced *Rückensäge*, but stands out among its congeners because also the lateral flanks and extremities exhibit additional and unique thorny elements or large tubercle scales, suggestive of some kind of veritable integumentary armor. Comparable structures are not known for any other member of *Brookesia*, and so far, it is unknown what these integumentary appendages truly are. The principle aim of the present study was to identify the histological structure and three-dimensional (3D) tissue composition of the different elements of the integumentary armor of this intriguing leaf chameleon.

2 | MATERIALS AND METHODS

Four adult specimens of both sexes of *B. perarmata* from the Zoologische Staatssammlung München (ZSM 862/2000: snout-vent length [SVL] = 61 mm, ♂; ZSM 17/2006: SVL = 60 mm, ♂; ZSM 914/2006: SVL = 59 mm, ♀; ZSM 915/2006: SVL = 52 mm, ♂) were analyzed for the present study. The specimens were kept preserved in ethanol according to standard museum procedures prior to this study.

One complete specimen (ZSM 17/2006) was scanned submersed in ethanol using a phoenix nanotom m (GE Measurement and Control) µCT-system with the following settings: tube voltage = 110 kV; tube current = 70 µA; target = tungsten, no filter; total sample rotation = 360°; angular step size = 0.24°; exposure time = 750 ms; binning = 1; averaging = 4; voxel size = 37.8 µm. The tomographic reconstruction was performed with the phoenix datos|x 2.2 software and converted to 8 bit in VG Studio 2.2. Digital rotation and cropping of the resulting image stack was performed in ImageJ (Schindelin et al., 2012) and textured mesh objects were extracted in Drishti 2.6.4 (Limaye, 2012). Final renderings were created in Blender 2.79 (blender.org). Using Daz Studio 4.10 (Daz Productions, Inc, Salt Lake City, UT), a reduced version of the digital hard tissue model was converted into a *.u3d file and embedded into an interactive 3D PDF by a custom LaTeX script.

Samples from the vertebrae, the skin of the lateral flanks, and anterior extremities containing both larger and smaller elements of the putative integumentary armor of the three other specimens were removed for histological analysis using a scalpel and forceps while keeping the entire specimens intact. The removed samples were transferred to 5% nitric acid. They were kept in this solution for about 48–60 hr to decalcify the tissue. Afterwards the samples were washed under running tap water for about 2 hr and returned to 70% ethanol. In addition, we took a sample of the skin of the lateral body wall devoid of any conspicuous armored elements for comparison.

Samples were dehydrated in ethanol and embedded in glycol methacrylate (Technovit 7,100, Heraeus Kulzer GmbH). The methacrylate blocks were sectioned at a thickness of 2–5 µm using a HM 350 rotary microtome (Microm International GmbH). The sections were stretched on a water bath and transferred to regular glass slides. Staining was done with a solution of 0.1% toluidine blue in 0.1% borax and the slides were cover-slipped using Roti Histokitt II (Carl Roth GmbH + Co. KG). Staining time varied according to section thickness and we furthermore produced, with regard to the soft tissues, overstained preparations as those yielded better results for the osseous parts contained in several of the sections. All analyses and imaging was done using a Zeiss Axio Lab.A1 light microscope equipped with a Canon EOS 60D digital camera. The resulting images were processed using RawTherapee 5.4 and GIMP 2.8 (adjustments of white balance, contrast, slight color adjustments and the removal of the background).

One additional isolated armored element of the lateral flanks was removed from each ZSM 862/2000 and ZSM 914/2006 as described above, dehydrated in a graded series of ethanol and finally transferred to and immersed in hexamethyldisilazane (HMDS) for 10 min (Nation, 1983). The samples were air-dried overnight and placed in separate sealed containers filled with silica gel the next morning and kept there until further analysis for about a week.

The dry sample from ZSM 914/2006 was embedded in Araldite® 2020 (Huntsman), cut with an IsoMet™ Low Speed Precision Cutter (Buehler), and ground with silicon carbide powder to produce petrographic ground sections. These sections were analyzed using a Leica DM LP polarizing microscope equipped with a Leica DFC 420 camera and further digitally processed as described for the conventional histological sections above.

Following the approach introduced by Rühr and Lambertz (2019), the dry sample from ZSM 862/2000 was gold-coated with a

108 auto sputter coater (Cressington Scientific Instruments) prior to μCT-scanning using a Skyscan 1272 device (Bruker microCT). The sputter-coating was required because the absorption indices of the sample's substructures differed so strongly that it was impossible to visualize the skin in the subsequent analysis steps. At high tube energies (>60 kV), the skin did not absorb enough photons to be visualized, while at lower energies (30–60 kV), the absorption of the underlying structure was so strong that its blurred outlines overlaid the weak skin signal in the digital slice reconstructions. The final μCT scan of the gold-coated sample was carried out with the following settings: tube voltage = 70 kV; tube current = 142 μA; target = tungsten; total sample rotation = 180°; angular step size = 0.19°; exposure time = 1925 ms; binning = 2 × 2; filter = Al 0.5 mm; averaging = 8; random movement = 15; voxel size = 4.4 μm. Thermal drift correction and digital section reconstruction was done in NRecon 1.7 (Bruker microCT). Textured mesh creation of the skin and the osteoderm, final rendering and 3D PDF creation procedures were carried out as described above for the whole body scan. Additionally, a digital endocast of the observed cavernous structure was generated with the region competition algorithm of ITK-SNAP (Yushkevich et al., 2006).

3 | RESULTS

3.1 | Macroscopic morphology

The macroscopic morphology of the integumentary armor in *B. perarmata* is illustrated by the digital reconstruction of a full-body μCT scan (Figure 1). The *Rückensäge* is formed by the dorsal vertebrae, which are modified as described in the following. The zygapophyses of the vertebrae rest on short, slightly outward projecting protrusions. The protrusions of the pre- and postzygapophysis are longitudinally connected by an osseous bridge forming a passage that is medially bordered by the centrum. These bridges also give rise to a long, broad, and laterally extending process. Originating from the anterior part of the longitudinal bridge, additional arches on either side are projecting dorso-caudad. These accessory arches merge dorsally and extend caudad to meet the dorsal tip of the neural spine, forming a shallow V-shape in dorsal view.

Aside from the cranial, axial, and appendicular skeleton, also the conspicuous tubercle scales on the lateral flanks and extremities appear as x-ray-dense structures with an absorbance similar to bone. Large tubercles are arranged in one longitudinal row along the flanks at about the dorso-ventral midline, whereas additional, smaller tubercles are scattered more ventrally. Both larger and smaller tubercles are rather cone-shaped in principle, but each of these cones consists of several minor cusps. The tubercles on the limbs are located proximal to the knee and elbow joints, respectively. Tubercles of the forelimb form a half-open bracelet with more numerous cusps, whereas those of the hindlimb again are more scattered and closer resemble the shape of those of the lateral flanks.

FIGURE 1 *Brookesia perarmata*, macroscopic view. Adult individual in life (a); skeletal reconstruction in lateral (b), with the right side digitally removed, and dorsal view (c). Note the osseous elements along the lateral flanks and the proximal extremities. Scale bar equals 1 cm. To view an interactive 3D model (PDF version only), click on the Figure. Standard views available in toolbar at the top. Additional mouse controls: Left click: rotate scene; right click / mouse wheel: zoom; both mouse buttons: pan. Figure best viewed with Adobe Acrobat Reader Version 9 or later

3.2 | Histology

3.2.1 | Vertebrae

The accessory structures of the vertebrae consist of bony tissue. Parts of the epaxial musculature run enclosed between the accessory arch and the neural spine (Figure 2a,b). A thick layer of cartilage covers the joint surfaces of the zygapophyses of adjacent vertebrae (Figure 2a,c). Both lateral processes and accessory arches are ornamented and spiny. In the caudal portion of the vertebrae, the arches and processes are almost completely compact (Figure 2a). Anterior to the neural spine, the lateral processes and accessory arches consist of a compact cortical layer hollowed out by interconnecting cavities filled by cavernous bone marrow (Figure 2b). The walls of the cavities are lined by secondary infillings with a regular, lamellar appearance. Osteocyte-lacunae are well visible throughout the lateral processes and accessory arches, but seem to be more numerous around the cavities. Potential growth marks are present within the vertebrae and seem to be continuous between the neural arches and the lateral processes, and continue further also into the accessory

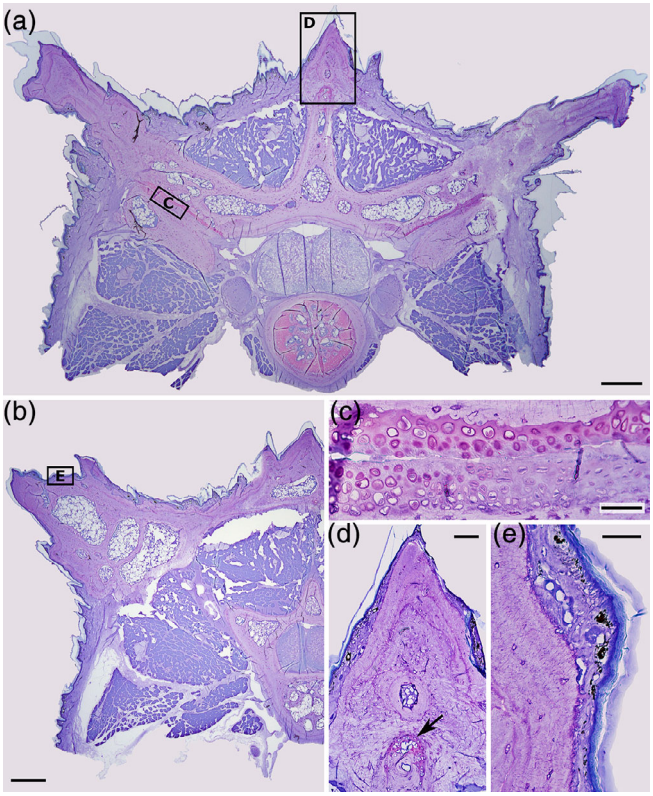

FIGURE 2 *Brookesia perarmata*, vertebral histology. Cross section of the last dorsal vertebra in a posterior plane (a) and hemi-section at about its midpoint (b). Note the cartilaginous zygapophyseal joint with the adjacent vertebra (c). The externally visible dorsal projection (d) shows a small island of cartilage at its base, just dorsal to the neural spine (arrow). The entire accessory, nontypical vertebral structures bulge out the dermis (e), which causes the external visibility. Scale bars equal 500 μm in a and b, 50 μm in c and e, and 100 μm in d

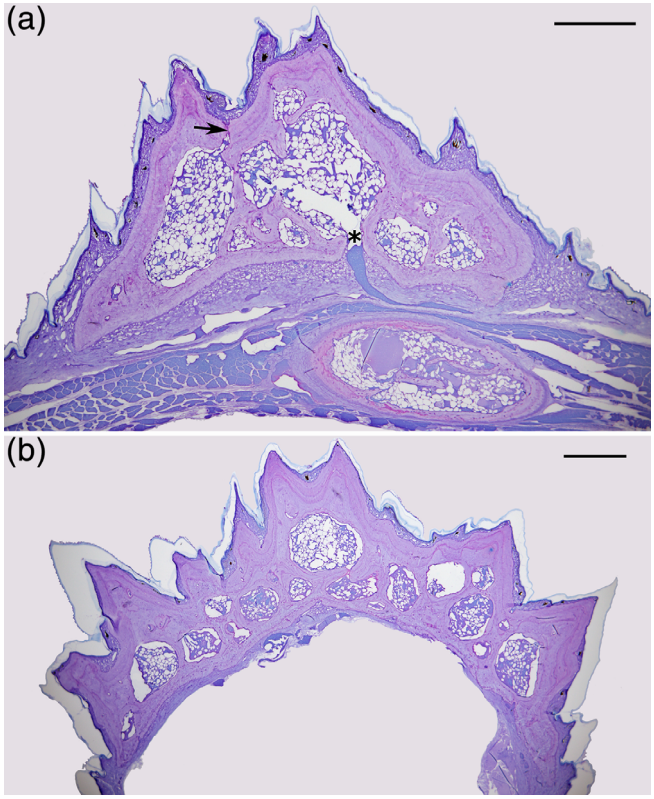

FIGURE 3 *Brookesia perarmata*, histological comparison of the integumentary armor. Both the armored elements of the lateral flanks (a, resting on the lateral body wall immediately above a rib) and those of the extremities (b) show the same principal architecture, most notably characterized by the osseous element (osteoderm) containing numerous large internal cavities. Note the larger blood vessels penetrating the bone at its basal (medial) side (asterisk) as well as the smaller ones at its superficial (lateral) one (arrow). All scale bars equal 500 μm

arches (Figure 2a,b). Growth lines, however, are not continuous where the accessory arches merge with the neural spine (Figure 2a,d). An additional patch of cartilage is found at the merging point of the accessory arches and the neural spine (Figure 2d). No discrete sutures, however, can be distinguished between the vertebra itself and any of its accessory structures (Figure 2a,b). Both the lateral processes and the accessory arches bulge out the skin and extend into the dermis, where they are covered by the dermal *stratum superficiale* and the overlying epidermis (Figure 2a,b,d,e).

3.2.2 | Normal skin of the lateral flanks

The skin is divided into a dermis and an epidermis. The dermis is divided into a basal *stratum compactum* of more regularly arranged collagen fibers and a *stratum superficiale* of irregular connective tissue. Numerous pigment cells are present in the apical regions of the *stratum superficiale*. The overlying, multilayered epidermis is covered by a micro-ornamented *Oberhäutchen*.

3.2.3 | Armor-like elements of the lateral flanks

The histological structure of the integument immediately surrounding the armor-like element of the lateral flanks agrees with the condition for the normal skin described above. The tubercle scale itself consists of an osseous core that is embedded within the *stratum superficiale* of the dermis and fully enveloped by it (Figures 3a and 4a). As on the rest of the body, the *stratum superficiale* covering the osseous core is scattered with various pigment cells and apically overlain by the epidermis (Figure 4b). The *stratum compactum* underneath the osseous element shows large, hollow lacunae reminiscent of vascular or lymphatic spaces (Figure 3a). Large blood vessels penetrate the bone from the basal (medial) side and extend into large, interconnected cavities (Figures 3a and 4c). These cavities are filled with marrow-like tissue that—albeit imperfectly preserved in the museum specimens—exhibits frequent vascular *sinus*, adipose cells, and a matrix of unidentifiable cells (Figure 4d). Smaller blood vessels penetrate the bone from the superficial (lateral) side and extend into the internal cavities (Figure 3a). The bony element itself consists of a compact cortical layer with mostly

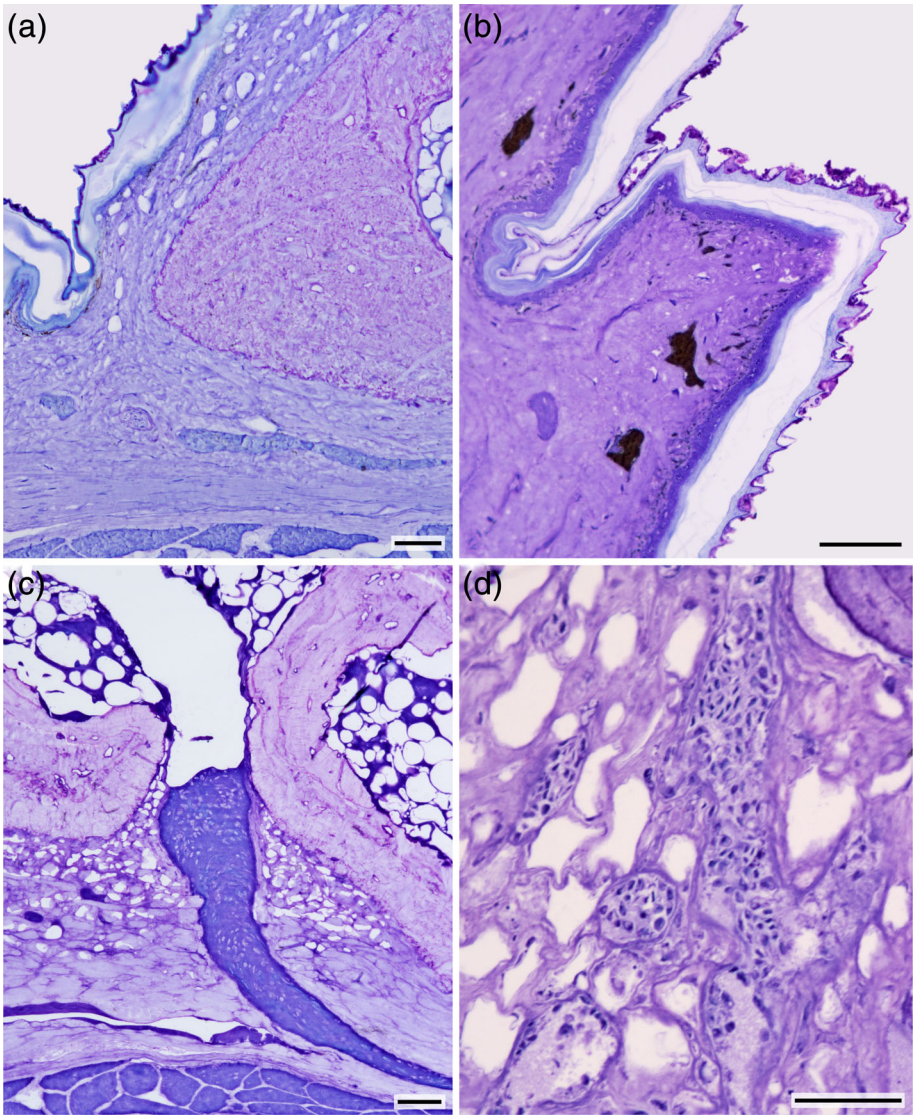

FIGURE 4 *Brookesia perarmata*, histological details of the lateral flank integumentary armor. Note that the osteoderm is fully enveloped by the *stratum superficiale* of the dermis (a), whereas the superficial dermal and epidermal layers resemble the ordinary squamate condition (b). Large blood vessels on the basal (medial) side (c) are, just as smaller ones on the superficial (lateral) side (not shown, but see arrow in Figure 3), connected to a marrow-like, potentially haematopoetic tissue within the osteoderm's cavities (d). All scale bars equal 50 μm

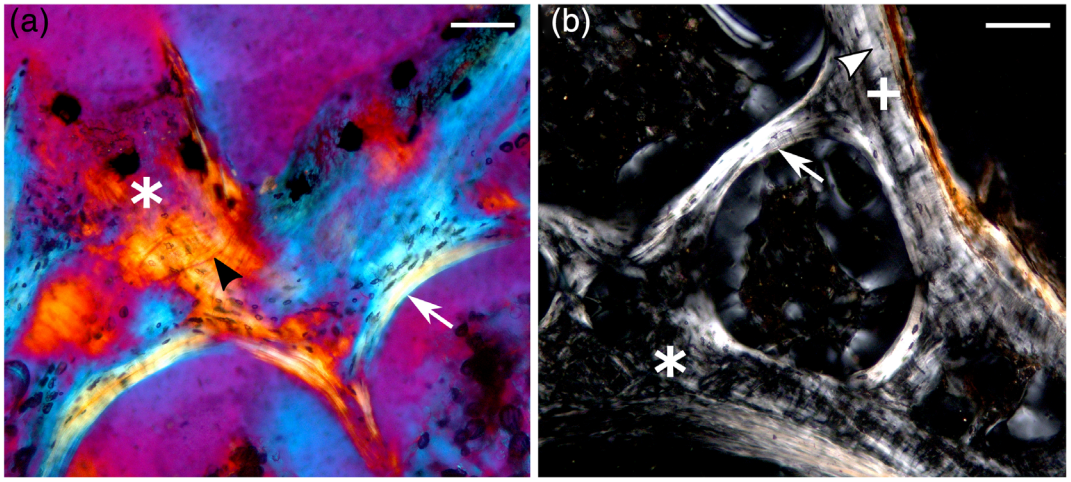

FIGURE 5 *Brookesia perarmata*, polarized microscopy of the lateral flank osteoderm. Note the remarkably complex architecture of the bone that is composed of parallel-fibered (plus sign), metaplastic (asterisk), and secondary lamellar bone (arrow). Fibers (black arrowhead) anchor the osteoderm within the dermis. At least one growth mark (white arrowhead) is visible in the parallel-fibered portion of the cortex. All scale bars equal 100 μm

rounded, osteocyte-lacunae dispersed throughout; canaliculi are well visible (Figure 5). Several potential growth marks are discernible (Figure 3a). Overall, the bone architecture of the central element displays a high complexity. Several parts of the peripheral cortex show a rather irregular arrangement of collagen fibers, comparable to that of the surrounding *stratum superficiale* (Figure 2a), and are indicative of metaplastic bone. The inner walls around the cavities are lined by secondary infillings with a more regular, lamellar appearance bordered by a cement line. There are both primary and secondary trabeculae. Bone and irregular connective tissue are interconnected by collagen bundles crossing from bone to dermis (Figure 5).

3.2.4 | Armor-like elements of the anterior extremities

The histological structure of the integument surrounding the armor-like element of the extremities again agrees with the condition for the normal skin of the flanks described above. In addition, also the histological composition of the armor-like element itself agrees with those of the flanks: a *stratum superficiale*-embedded, multicusped, osseous element containing numerous cavities filled with marrow-like tissue. The above-mentioned shape reminiscent of a half-open bracelet is clearly evident (Figure 3b).

3.3 | 3D-morphology of the lateral flank integumentary armor

The central bony element of the lateral flank armor can clearly be separated from the surrounding soft tissue of the skin in the μCT scans (Figure 6a). The osseous core directly resembles that of the externally visible, cone-shaped structure with its several minor cusps of the "tubercle scale" itself (Figure 6a,b). There are numerous larger vascular foramina on the basal (medial) face of the osseous core, and several smaller ones on the superficial (lateral) side (Figure 6b,c; see also Figures 3a and 4c). The cavities within the bone are all connected with each other (Figure 6d), which became evident due to the fact that the semiautomatic reconstruction employed produced a complete and continuous "endocast" after several starting points were set in the central portion of the osteoderm.

4 | DISCUSSION

The macroscopic external appearance of the conspicuous putative body armor of *Brookesia perarmata* has been known since the original description of this species by Angel (1933). We were able to corroborate the osteological findings on the vertebral projections in *B. superciliaris* by Siebenrock (1893) and Parker and Taylor (1942) also for the Antsingy leaf chameleon. A bridge-like arch extends between the pre- and postzygapophyses, connects both of them, projects laterally, and extends into the dermis.

These also externally visible projections constitute unique structural elements not known for any other lepidosaur outside the genus *Brookesia* and contribute to generating the appearance of body armor. The question remains though how they are formed. Romer (1956), without further elaborating, which species he examined nor how he came to this conclusion, considered them as "[s]uperficial dermal ossification[s]" (p. 539). Our histological analyses revealed continuous growth lines and the absence of discrete sutures for the lateral

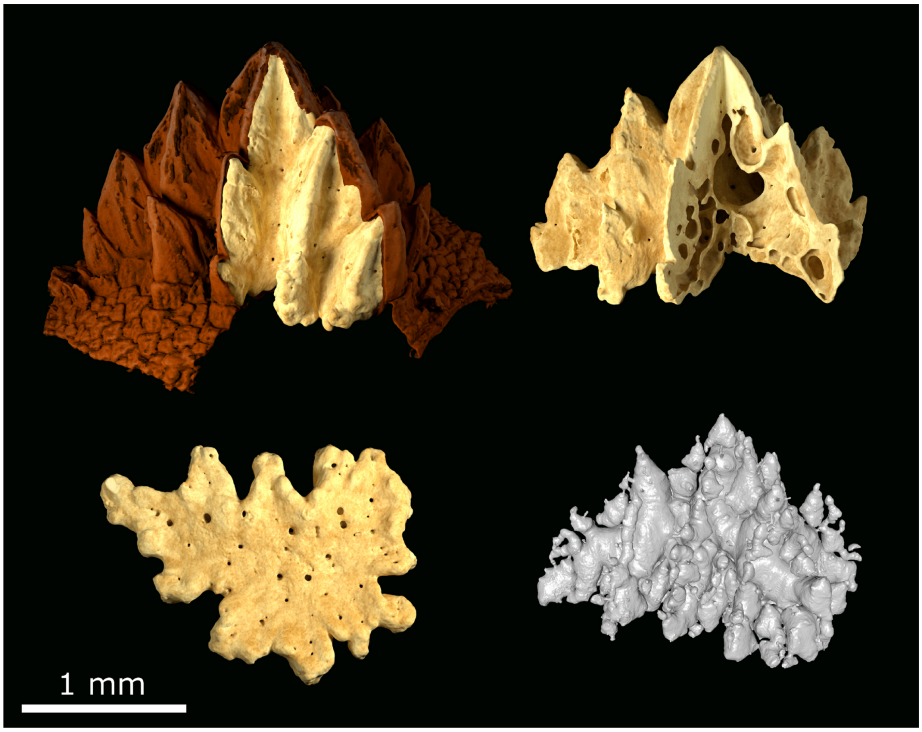

FIGURE 6 *Brookesia perarmata*, 3D-reconstruction of the lateral flank integumentary armor of *Brookesia perarmata*. Note that the shape of the multicusped osteoderm directly reflects the external morphology of the tubercle scale (a, b) and that there are numerous smaller superficial (lateral) and larger basal (medial) vascular canals within the bone (b, c). All the internal cavities are connected to each other (d). Scale bar equals 1 mm. To view an interactive 3D model (PDF version only), click on the Figure. Standard views available in toolbar at top. Individual meshes of skin, bone and endocast of osteoderm can be toggled on/off when "Model Tree" is activated in tool bar. Additional mouse controls: Left click: rotate scene; right click/ mouse wheel: zoom; both mouse buttons: pan. Figure best viewed with Adobe Acrobat Reader Version 9 or later

projections with the vertebral body, suggesting that the vertebrae and these accessory structures in fact form a developmental unity. Dorsally, however, the externally visible projection appears to be somewhat separable from the dorsal tip of the vertebral neural spine in terms of its bone architecture, and the presence of cartilaginous remnants may be suggestive of a fusion of two discrete structures. Based on the material available to us, we can neither rule out that the accessory structures are of dermal origin fusing with the vertebrae, nor that they form as endochondral ossification and as outgrowths of the vertebrae themselves, or even that it is a combination of both processes. In order to unambiguously answer the question of developmental origin, ontogenetic studies based on an appropriate series of specimens at different ages seem ultimately needed.

Turning to the thorny elements of the lateral flanks and extremities of *B. perarmata*, we see different general macroscopic shapes, but a corresponding histological architecture. Both do not represent mere keratinous tubercle scales, but rather exhibit a multicusped osseous core. The location of these bony elements embedded within the dermis warrants their interpretation as osteoderms. No such structures are known for any other species of chamaeleonid, including the numerous congeners. To the best of our knowledge, this is the first known case for the presence of osteoderms for any member of the Chamaeleonidae and, except for the marine iguana, *Amblyrhynchus cristatus* Bell, 1825 (see de Queiroz, 1987), only the second for the entire clade Iguania.

Osteoderms are known for a number of tetrapod lineages, but among lepidosaurs they were so far considered to be restricted to anguids (de Buffrénil, Sire, & Rage, 2010; Moss, 1969; Schmidt, 1914a; Strahm & Schwartz, 1977), anniellids (Bhullar & Bell, 2008), cordylids (Broeckhoven, El Adak, Hui, Van Damme, & Stankowich, 2018; Romer, 1956; Stanley, 2013), gekkotans (Laver et al., 2020; Levrat-Calviac, Castanet, & Zylberberg, 1986; Levrat-Calviac & Zylberberg, 1986; Paluh, Griffing, & Bauer, 2017; Schmidt, 1912a; Vickaryous, Meldrum, & Russell, 2015), gerrhosaurids (Moss, 1969; Schmidt, 1912b), helodermatids (Mead, Schubert, Wallace, & Swift, 2012; Moss, 1969; Schmidt, 1912c), lacertids (Costantini, Alonso, Moazen, & Bruner, 2010; Gadow, 1909), lanthanotids (Maisano, Bell, Gauthier, & Rowe, 2002), scincids (Lambiris, 1992; Moss, 1969; Schmidt, 1910), shinisaurids (Bever, Bell, & Maisano, 2005; Conrad, Head, & Carrano, 2014), varanids (Erickson, Ricqles, de Buffrénil, Molnar, & Bayless, 2003; Maisano, Laduc, Bell, & Barber, 2019), xenosaurids (Bhullar, 2011), and, as already mentioned, the iguanid *A. cristatus* (de Queiroz, 1987).

While the normal skin in the Antsingy leaf chameleon follows the general morphology of the squamate integument, the osteoderms themselves are rather unusual. Osteoderm morphology differs greatly within squamates, not only in relation to shape, size and distribution on the body (Paluh et al., 2017; Vickaryous & Sire, 2009), but also with respect to tissue composition (Vickaryous et al., 2015; Vickaryous & Sire, 2009). Most frequently, osteoderms are limited to the dorsal surface of the head and trunk (Gadow, 1909), whereas in other taxa (e.g., anguids, some gekkotans, and scincids) they enclose the entire body (Vickaryous et al., 2015; Vickaryous & Sire, 2009). In many squamate taxa, osteoderms are relatively small or thin (Otto, 1909; Paluh et al., 2017) and do not change or influence the outer silhouette of the animal. Even though their distribution is much more localized in *B. perarmata*, the osteoderms are conspicuous and large compared with the animal's size and, especially in combination with the *Rückensäge*, dramatically alter its body contour. Osteoderm shape ranges from vermicular in varanids (Erickson et al., 2003), imbricating and flat in anguids and scincids (Levrat-Calviac et al., 1986; Otto, 1909; Schmidt, 1910, 1914a), to robust and bead-like in helodermatids (Mead et al., 2012; Vickaryous & Sire, 2009), or elongated with branching processes in anniellids (Bhullar & Bell, 2008). However, large, conical, and multicusped osteoderms such as those of *B. perarmata* seem to be exceptional.

Vickaryous and Sire (2009) found that in all lepidosaurians they investigated, osteoderms were embedded into the dermis directly at the juncture of the *stratum superficiale* and *stratum compactum*. The osteoderms of *B. perarmata*, however, are completely enveloped by the *stratum superficiale*, so that there is no contact with the *stratum compactum*. Though fundamentally different with regard to the osteoderm structure itself, this is reminiscent of the condition found in *Geckolepis maculata* Peters, 1880 (Paluh et al., 2017).

For the gecko *Tarentola mauritanica* (Linnaeus, 1758), Levrat-Calviac and Zylberberg (1986) described bundles of collagen fibers comparable to Shapey's fibers anchoring the osteoderms within the dermis, and Vickaryous et al. (2015) confirmed this interpretation. Corresponding fibers are also present in *B. perarmata* and appear to secure the osteoderm within the surrounding superficial dermis.

Tissue composition of squamate osteoderms also varies greatly and is by no means restricted to osseous components, comprising a diverse spectrum of other mineralized and unmineralized tissues (Moss, 1969; Vickaryous & Sire, 2009). As a rough generalization, two types of osteoderms can be distinguished: (a) those that (at least primarily) consist of bone (e.g., in *Anguis fragilis* Linnaeus, 1758 and some gekkonids) (Vickaryous et al., 2015; Zylberberg & Castanet, 1985), and (b) those that additionally contain a mostly avascular and acellular, hypermineralized dental-like tissue (de Buffrénil et al., 2010; Iacoviello et al., 2020; Levrat-Calviac & Zylberberg, 1986; Moss, 1969; Vickaryous et al., 2015), recently termed osteodermine (de Buffrénil, Dauphin, Rage, & Sire, 2011). The osteoderms of *B. perarmata* clearly fall into the former category. But in contrast to, for instance, *A. fragilis* in which the osteoderms are divided into a basal layer of lamellar bone and a superficial layer of woven-fibered bone (Zylberberg & Castanet, 1985), the osteoderms of the Antsingy leaf chameleon do not show such a two-part organization and lamellar bone is only found around the inner cavity walls.

Generally, reptilian dermal bone rarely possesses any cavities and is rather poorly vascularized (Moss, 1969). Schmidt (1910, 1912a, 1912b, 1912c, 1914a) noted the presence of small vascular canals for gekkotans, gerrhosaurids, scincids, helodermatids, and anguids. For *Gerrhosaurus* Wiegman, 1828 and *Zonosaurus* Boulenger, 1887, Schmidt (1912b) also described small cavities ("*Markräume*"), probably resulting from resorption, but did not provide further information about the soft tissue

occupying these spaces. As a generalized remark, Moss (1969) stated that, if present, cavities were filled by fat cells and hematopoietic tissue, but he did not mention differences between the taxa he investigated. Otto (1909) reported small cavities in the osteoderms of *Chalcides chalcides* (Linnaeus, 1758) and *C. ocellatus* (Forskål, 1775). He interpreted the internal tissue as vascularized adipose cells, possibly combined with connective tissue and pigment cells. More recently, Broeckhoven, du Plessis, and Hui (2017) described well-vascularized osteoderms exhibiting cavities filled with adipose tissue in a cordylid. However, and despite a superficial similarity, the osteoderms of *B. perarmata* with their large, interconnecting cavities filled by what appears to be bone marrow remain remarkable. The closest superficial resemblance may actually be found in the osteoderms of certain fossil glyptosaurine anguids, which exhibit a diploe structure with relatively large cavities, even though these spaces are most pronounced in the cranial region and it remains uncertain what these were filled with in the living animal (de Buffrénil et al., 2010).

The medullary region of *B. perarmata*'s osteoderms shows considerable areas of resorption and redeposition with secondary infillings of lamellar bone bordered by a cement line along the trabeculae and inner walls of the cavities. In reptiles, the formation of lamellar bone is considered to require the presence of a periosteum (Moss, 1969; or endosteum), which would indicate a formation by intramembranous ossification. Except for secondary infillings, collagen arrangement within the osteoderms of *B. perarmata* is rather irregular and directly continuous with that of the surrounding superficial dermis, which, on the other hand, suggests a formation by metaplasia (Haines & Mohuiddin, 1968; Levrat-Calviac & Zylberberg, 1986; Moss, 1969). These findings may indicate that osteoderm formation in *B. perarmata* is achieved by a combination of intramembranous ossification and metaplasia, which would be in congruence with the current knowledge for Lepidosauria in general (Vickaryous & Sire, 2009).

The general structure of the Antsingy leaf chameleon's osteoderms can be characterized as somewhat “spongy” and thus at least superficially resembles that of crocodylian osteoderms (see also those of the South American horned frogs, Quinzio & Fabrezi, 2012). Osteoderm coverage in crocodylians is extensive, and depending on the species is not restricted to the dorsolateral surface but also extends to the ventral abdomen (Schmidt, 1914b; Vickaryous & Hall, 2008). Crocodylian osteoderms are more or less disc like and often possess a central protuberance or keel and apical ornamentation (Vickaryous & Hall, 2008). Microstructurally, crocodylian osteoderms exhibit a distinct diploe structure consisting of a compact cortex and a cancellous central portion (de Buffrénil et al., 2015; Vickaryous & Sire, 2009) similar to that found in *B. perarmata*. In contrast to most lepidosaurians, crocodylian osteoderms lie within the *stratum superficiale* and are anchored by Sharpey's fibers (de Buffrénil et al., 2015; Vickaryous & Sire, 2009), again reminiscent of the situation in *B. perarmata*. Apical and basal sides of crocodylian osteoderms are penetrated by small neurovascular foramina (Schmidt, 1914b; Vickaryous & Hall, 2008), but cavities are not limited to vascular spaces alone (Schmidt, 1914b). Schmidt (1914b) found that, at least in *Crocodylus niloticus* Laurenti, 1768, cavities were filled by a combination of connective tissue, blood vessels, nerves, and pigment cells. In contrast to that, the cavities of the osteoderms in *B. perarmata* appear to lack pigment cells, but are filled by potential hematopoietic tissue. Crocodylian osteoderms are composed of a mixture of woven bone, parallel-fibered bone, lamellar bone, and mineralized and unmineralized connective tissue (de Buffrénil et al., 2015; Vickaryous & Hall, 2008). While Vickaryous and Hall (2008) did not find signs of intramembranous ossification in *Alligator mississippiensis* (Daudin, 1802) and consider bone metaplasia to be the only mode of osteoderm formation in crocodylians, de Buffrénil et al. (2015) investigated numerous extant and fossil Crocodylomorpha and found endosteal bone deposits in older (i.e., larger) individuals suggestive of osteoblast activity. As already stated, a similar combination of metaplasia and intramembranous ossification might also be present in *B. perarmata*. However, all of this taken together, renders the osteoderm morphology of the Antsingy leaf chameleon quite remarkable and unique among lepidosaurs, and thus expands our knowledge about the structural diversity of the amniote integument.

Concerning the functional significance of these structures for *B. perarmata*, the situation is even more confounded. Traditionally, reptilian osteoderms have been regarded solely as defensive structures, that is, dermal armor in the literal sense. However, even though this might be true for some taxa, it does not explain the occurrence of relatively thin and fragile osteoderms (Broeckhoven, Diedericks, & Mouton, 2015; Paluh et al., 2017). More recent hypotheses widen the presumed function of osteoderms. Vickaryous et al. (2015) proposed a possible protection during aggressive intraspecific behavior as well as against well-fortified, large prey items in several species of geckos. Dacke et al. (2015) studied labile calcium sources in reproducing alligators and suggested that osteoderms serve as calcium deposits for eggshell production. A similar function as mineral reservoirs has also been discussed for sauropod dinosaur osteoderms (Curry Rogers, D'Emic, Rogers, Vickaryous, & Cagan, 2011). Furthermore, a possible role in thermoregulation in crocodilians and squamates has been discussed by several authors (Broeckhoven et al., 2017; Clarac, de Buffrénil, Cubo, & Quilhac, 2018; Clarac & Quilhac, 2019; Drane & Webb, 1980; Vickaryous & Hall, 2008; Vickaryous & Sire, 2009). For *B. perarmata*, no information on thermoregulation and calcium metabolism is available (although it is restricted to karstic limestone habitats), therefore a possible influence of such physiological processes on osteoderm advantageousness can hardly be discussed.

In his work on *B. superciliaris*, Siebenrock (1893) interpreted the accessory arches and zygapophyseal bridges of the vertebrae as strengthenings of the vertebral column, and considered the lateral spines as adornments (“*Zierde*”; possibly in the sense of display structures). The fact that both males and females of the species exhibit these armor-like elements appears to contradict the hypothesis of a display structure that would play a signaling role during mating

behaviors. However, we cannot exclude a simultaneous visual and mechanical function, and especially the potential for bone-based fluorescence known for other chameleons warrants further examination (Prötzel et al., 2018).

Chameleons mainly rely on camouflage and crypsis to avoid predation, and leaf chameleons are no exception. The *Rückensäge* and osteoderms could actually facilitate such a strategy. In addition, Raxworthy (1991) documented that at least some *Brookesia* species not only rely on passive defense behavior when gripped, but switch to active vibrating or even thrusting of the dorsolateral-spines to deter predators. It is conceivable that *B. peramata* may use both, the pointed osteoderms and dorsolateral-spines, in such a spine thrusting response.

Birds and snakes have been identified as the main predators for Malagasy chameleons, and specifically several *Brookesia* serve as a substantial dietary component of for instance the short-legged ground roller (Jenkins, Rabearivony, & Rakotomanana, 2009). Against avian and ophidian predators, the exceptional osteoderms of *B. perarmata* in fact may contribute toward their general defense strategy. All species of *Brookesia* exhibit a somewhat sculptured skull presenting several prominent crests that may be harmful to potential predators trying to swallow them in one piece. The same applies to the vertebral projections of the *Rückensäge* that is characteristic for most species of the genus. The entire physiognomy of the Antsingy leaf chameleon with its pronounced "spikyness" over larger parts of the body, as a result of the numerous large osteoderms, may enhance such effects.

ACKNOWLEDGMENTS

P. Martin Sander and Olaf Dülfer are thanked for providing access to the bone histology laboratory, as well as for helpful discussions. We are grateful to the Malagasy authorities for research, collection, and export permits, and to the German authorities for import permits.

AUTHOR CONTRIBUTIONS

Pia Schucht: Formal analysis; investigation; visualization; writing-original draft. **Peter Rühr:** Formal analysis; visualization; writing-review and editing. **Benedikt Geier:** Visualization; writing-review and editing. **Frank Glaw:** Conceptualization; writing-review and editing. **Markus Lambertz:** Conceptualization; formal analysis; investigation; methodology; project administration; writing-original draft.

CONFLICT OF INTEREST

The authors declare that there is no conflict of interests.

DATA AVAILABILITY STATEMENT

The data that support the findings of this study can be accessed at Zenodo (doi: 10.5281/zenodo.3716103).

ORCID

Pia J. Schucht https://orcid.org/0000-0002-8853-3092
Peter T. Rühr https://orcid.org/0000-0003-2776-6172
Benedikt Geier https://orcid.org/0000-0002-2942-2624
Markus Lambertz https://orcid.org/0000-0001-8348-9347

REFERENCES

Angel, F. (1933). Sur un genre Malgache nouveau, de la famille des Chamaeléontidés. *Bulletin du Muséum d'Histoire Naturelle Paris*, *5*, 443–446.

Bell, T. (1825). On a new genus of Iguanidae. *Zoological Journal*, *2*, 204–208.

Best, A. E. (1968). The discovery of the mechanism of colour-changes in the chameleon. *Annals of Science*, *24*, 147–167.

Bever, G. S., Bell, C. J., & Maisano, J. A. (2005). The ossified braincase and cephalic osteoderms of *Shinisaurus crocodilurus* (Squamata, Shinisauridae). *Palaeontologia Electronica*, *8*, 1–36.

Bhullar, B. A. S. (2011). The power and utility of morphological characters in systematics: A fully resolved phylogeny of *Xenosaurus* and its fossil relatives (Squamata: Anguimorpha). *Bulletin of the Museum of Comparative Zoology at Harvard College*, *160*, 65–181.

Bhullar, B. A. S., & Bell, C. J. (2008). Osteoderms of the California legless lizard *Anniella* (Squamata: Anguidae) and their relevance for considerations of miniaturization. *Copeia*, *2008*, 785–793.

Boettger, O. (1878). Die Reptilien und Amphibien von Madagascar. Zweiter Nachtrag. *Abhandlungen der Senckenbergischen Naturforschenden Gesellschaft*, *11*, 457–497 + 1 pl.

Boettger, O. (1893). *Katalog der Reptilien-Sammlung im Museum der Senckenbergischen Naturforschenden Gesellschaft in Frankfurt am Main. I. Teil (Rhynchocephalen, Schildkröten, Krokodile, Eidechsen, Chamäleons)*. Frankfurt a. M.: Gebrüder Knauer.

Boistel, R., Herrel, A., Daghfous, G., Libourel, P. A., Boller, E., Tafforeau, P., & Bels, V. (2010). Assisted walking in Malagasy dwarf chamaeleons. *Biology Letters*, *6*, 740–743.

Boulenger, G. A. (1887). *Catalogue of the lizards in the British museum (natural history)* (2nd ed.). London: Printed by order of the Trustees.

Broeckhoven, C., Diedericks, G., & Mouton, P. L. F. N. (2015). What doesn't kill you might make you stronger: Functional basis for variation in body Armour. *Journal of Animal Ecology*, *84*, 1213–1221.

Broeckhoven, C., du Plessis, A., & Hui, C. (2017). Functional trade-off between strength and thermal capacity of dermal armor: Insights from girdled lizards. *Journal of the Mechanical Behavior of Biomedical Materials*, *74*, 189–194.

Broeckhoven, C., El Adak, Y., Hui, C., Van Damme, R., & Stankowich, T. (2018). On dangerous ground: The evolution of body Armour in cordyline lizards. *Proceedings of the Royal Society B: Biological Sciences*, *285*, 20180513.

Canham, M. T. (1999). The identification of specialized scale surface structures and scale arrangements of the ventral portion of a prehensile tail, used for increased rip in the *Chamaeleo* genus. *Chameleon Information Network*, *33*, 5–8.

Clarac, F., de Buffrénil, V., Cubo, J., & Quilhac, A. (2018). Vascularization in ornamented osteoderms: Physiological implications in ectothermy and amphibious lifestyle in the crocodylomorphs? *The Anatomical Record*, *301*, 175–183.

Clarac, F., & Quilhac, A. (2019). The crocodylian skull and osteoderms: A functional exaptation to ectothermy? *Zoology*, *132*, 31–40.

Conrad, J. L., Head, J. J., & Carrano, M. T. (2014). Unusual soft-tissue preservation of a crocodile lizard (Squamata, Shinisauria) from the green river formation (Eocene) and shinisaur relationships. *The Anatomical Record*, *297*, 545–559.

Costantini, D., Alonso, M. L., Moazen, M., & Bruner, E. (2010). The relationship between cephalic scales and bones in lizards: A preliminary microtomographic survey on three lacertid species. *The Anatomical Record*, *293*, 183–194.

Curry Rogers, K., D'Emic, M., Rogers, R., Vickaryous, M., & Cagan, A. (2011). Sauropod dinosaur osteoderms from the late cretaceous of Madagascar. *Nature Communications*, *2*, 564.

Dacke, C. G., Elsey, R. M., Trosclair, P. L., Sugiyama, T., Nevarez, J. G., & Schweitzer, M. H. (2015). Alligator osteoderms as a source of labile calcium for eggshell formation. *Journal of Zoology*, *297*, 255–264.

Daudin, F. M. (1802). *Histoire Naturelle, Générale et Particulière des Reptiles. Tome Second*. Paris: F. Dufart.

de Buffrénil, V., Clarac, F., Fau, M., Martin, S., Martin, B., Pellé, E., & Laurin, M. (2015). Differentiation and growth of bone ornamentation in vertebrates: A comparative histological study among the Crocodylomorpha. *Journal of Morphology*, *276*, 425–445.

de Buffrénil, V., Dauphin, Y., Rage, J. C., & Sire, J. Y. (2011). An enamel-like tissue, osteodermine, on the osteoderms of a fossil anguid (Glyptosaurinae) lizard. *Comptes Rendus Palevol*, *10*, 427–437.

de Buffrénil, V., Sire, J. Y., & Rage, J. C. (2010). The histological structure of glyptosaurine osteoderms (Squamata: Anguidae), and the problem of osteoderm development in squamates. *Journal of Morphology*, *271*, 729–737.

de Queiroz, K. (1987). Phylogenetic systematics of iguanian lizards: A comparative osteological study. *University of California Publications in Zoology*, *118*, 1–203.

Drane, C. R., & Webb, G. J. W. (1980). Functional morphology of the dermal vascular system of the Australian lizard *Tiliqua scincoides*. *Herpetologica*, *36*, 60–66.

Erickson, G. M., Ricqles, A. D., de Buffrénil, V., Molnar, R. E., & Bayless, M. K. (2003). Vermiform bones and the evolution of gigantism in *Megalania*—How a reptilian fox became a lion. *Journal of Vertebrate Paleontology*, *23*, 966–970.

Forskål, P. (1775). *Descriptiones animalium avium, amphibiorum, piscium, insectorum, vermium*. Möller: Havniæ [Copenhagen].

Gadow, H. (1909). *Amphibia and reptiles*. London: Macmillan and Co., Limited.

Glaw, F. (2015). Taxonomic checklist of chameleons (Squamata: Chamaeleonidae). *Vertebrate Zoology*, *65*, 167–246.

Glaw, F., Hawlitschek, O., & Ruthensteiner, B. (2013). A new genus name for an ancient Malagasy chameleon clade and a PDF-embedded 3D model of its skeleton. *Salamandra*, *49*, 237–238.

Glaw, F., Köhler, J., Townsend, T. M., & Vences, M. (2012). Rivaling the world's smallest reptiles: Discovery of miniaturized and microendemic new species of leaf chameleons (*Brookesia*) from northern Madagascar. *PLoS One*, *7*, e31314.

Gray, J. E. (1865). Revision of the genera and species of Chamæleonidae, with the description of some new species. *Proceedings of the Zoological Society of London*, *1864*, 465–479.

Haines, R. W., & Mohuiddin, A. (1968). Metaplastic bone. *Journal of Anatomy*, *103*, 527.

Iacoviello, F., Kirby, A. C., Javanmardi, Y., Moeendarbary, E., Shabanli, M., Tsolaki, E., … Brett, D. J. (2020). The multiscale hierarchical structure of *Heloderma suspectum* osteoderms and their mechanical properties. *Acta Biomaterialia*, *107*, 194–203.

Jenkins, R. K. B., Rabearivony, J., & Rakotomanana, H. (2009). Predation on chameleons in Madagascar: A review. *African Journal of Herpetology*, *58*, 131–136.

Kuhl, H. (1820). *Beiträge zur Zoologie und vergleichenden Anatomie*. Hermannsche Buchhandlung: Frankfurt am Main.

Lambiris, A. (1992). Preliminary remarks on the use of osteoderms as an adjunct to the taxonomy of southern African lizards. *The Journal of the Herpetological Association of Africa*, *40*, 14–18.

Laurenti, J. (1768). *Specimen medicum, exhibens synopsin reptilium emendatam cum experimentis circa venena et antidota reptilium Austriacorum*. Vienna: Trattnern.

Laver, R. J., Morales, C. H., Heinicke, M. P., Gamble, T., Longoria, K., Bauer, A. M., & Daza, J. D. (2020). The development of cephalic armor in the tokay gecko (Squamata: Gekkonidae: *Gekko gecko*). *Journal of Morphology*, *281*, 213–228.

Levrat-Calviac, V., Castanet, J., & Zylberberg, L. (1986). The structure of the osteoderms in two lizards: *Tarentola mauritanica* and *Anguis fragilis*. In Z. Roček (Ed.), *Studies in herpetology: Proceedings of the European herpetological meeting* (pp. 341–344). Prague: Charles University Prague for the Societas Europaea Herpetologica.

Levrat-Calviac, V., & Zylberberg, L. (1986). The structure of the osteoderms in the gekko: *Tarentola mauritanica*. *Developmental Dynamics*, *176*, 437–446.

Ligon, R. A., & McGraw, K. J. (2013). Chameleons communicate with complex colour changes during contests: Different body regions convey different information. *Biology Letters*, *9*, 20130892.

Limaye, A. (2012). Drishti: a volume exploration and presentation tool. Proceedings of SPIE 8506, Developments in X-Ray Tomography VIII, 85060X.

Linnaeus, C. (1758). *Systema naturæ per regna tria naturæ, secundum classes, ordines, genera, species, cum characteribus, differentiis, synonymis, locis. Tomus I. Editio decima, reformata*. Holmiæ [Stockholm]: Laurentii Salvii.

Maisano, J. A., Bell, C. J., Gauthier, J. A., & Rowe, T. (2002). The osteoderms and palpebral in *Lanthanotus borneensis* (Squamata: Anguimorpha). *Journal of Herpetology*, *36*, 678–683.

Maisano, J. A., Laduc, T. J., Bell, C. J., & Barber, D. (2019). The cephalic osteoderms of *Varanus komodoensis* as revealed by high resolution X ray computed tomography. *The Anatomical Record*, *302*, 1675–1680.

Mead, J. I., Schubert, B. W., Wallace, S. C., & Swift, S. L. (2012). Helodermatid lizard from the Mio-Pliocene oak-hickory forest of Tennessee, eastern USA, and a review of monstersaurian osteoderms. *Acta Palaeontologica Polonica*, *57*, 111–121.

Moss, M. L. (1969). Comparative histology of dermal sclerifications in reptiles. *Cells, Tissues, Organs*, *73*, 510–533.

Nation, J. L. (1983). A new method using hexamethyldisilazane for preparation of soft insect tissues for scanning electron microscopy. *Stain Technology*, *58*, 347–351.

Otto, H. (1909). Die Beschuppung der Brevilinguier und Ascalaboten. *Jenaische Zeitschrift für Naturwissenschaft*, *44*, 193–252.

Paluh, D. J., Griffing, A. H., & Bauer, A. M. (2017). Sheddable Armour: Identification of osteoderms in the integument of *Geckolepis maculata* (Gekkota). *African Journal of Herpetology*, *66*, 12–24.

Parker, H. W., & Taylor, R. H. R. (1942). The lizards of British Somaliland. *Bulletin of the Museum of Comparative Zoology at Harvard College*, *91*, 1–101.

Peters, W. (1880). Über die von Hrn. J. M. Hildebrandt auf Nossi-Bé und Madagascar gesammelten Säugethiere und Amphibien. *Monatsberichte der königlich Preussischen Akademie der Wissenschaften Zu Berlin*, *1880*, 508–511.

Prötzel, D., Heß, M., Scherz, M. D., Schwager, M., van't Padje, A., & Glaw, F. (2018). Widespread bone-based fluorescence in chameleons. *Scientific Reports*, *8*, 698.

Quinzio, S., & Fabrezi, M. (2012). Ontogenetic and structural variation of mineralizations and ossifications in the integument within ceratophryid frogs (Anura, Ceratophryidae). *The Anatomical Record*, *295*, 2089–2103.

Raxworthy, C. J. (1991). Field observations on some dwarf chameleons (*Brookesia* spp.) from rainforest areas of Madagascar, with description of a new species. *Journal of Zoology*, *224*, 11–25.

Riedel, J., Böhme, W., Bleckmann, H., & Spinner, M. (2015). Microornamentation of leaf chameleons (Chamaeleonidae: *Brookesia*, *Rhampholeon*, and *Rieppeleon*)—With comments on the evolution of microstructures in the Chamaeleonidae. *Journal of Morphology*, *276*, 167–184.

Romer, A. S. (1956). *Osteology of the reptiles (Third impression 1976)*. Chicago & London: University of Chicago Press.

Rühr, P. T., & Lambertz, M. (2019). Surface contrast enhancement of integumentary structures in X-ray tomography. *Journal of Anatomy*, *235*, 379–385.

Schindelin, J., Arganda-Carreras, I., Frise, E., Kaynig, V., Longair, M., Pietzsch, T., … Cardona, A. (2012). Fiji: An open-source platform for biological-image analysis. *Nature Methods*, *9*, 676–682.

Schleich, H. H., & Kästle, W. (1985). Skin structures of Sauria extremities—SEM-studies of four families. *Fortschritte der Zoologie*, *30*, 99–101.

Schmidt, W. J. (1910). Das Integument von *Voeltzkowia mira* BTTGR. Ein Beitrag zur Morphologie und Histologie der Eidechsenhaut. *Zeitschrift für Wissenschaftliche Zoologie*, *94*, 605–720.

Schmidt, W. J. (1912a). Studien am Integument der Reptilien. I. Die Haut der Geckoniden. *Zeitschrift für Wissenschaftliche Zoologie*, *51*, 139–258.

Schmidt, W. J. (1912b). Studien am Integument der Reptilien. III. Über die Haut der Gerrhosauriden. *Zoologische Jahrbücher*, *Abteilung für Anatomie Und Ontogenie der Tiere*, *35*, 75–104.

Schmidt, W. J. (1912c). Studien am Integument der Reptilien. II. Hautverknöcherungen von *Heloderma*. *Zoologische Jahrbücher*, *Supplement*, *15*, 219–228.

Schmidt, W. J. (1914a). Studien am Integument der Reptilien: V. Anguiden. *Zoologische Jahrbücher*, *Abteilung für Anatomie Und Ontogenie der Tiere*, *38*, 1–102.

Schmidt, W. J. (1914b). Studien am Integument der Reptilien. VI. Über die Knochenschuppen der Crocodile. *Zoologische Jahrbücher*. *Abteilung für Anatomie und Ontogenie der Tiere*, *38*, 643–666.

Siebenrock, F. (1893). Das Skelet von *Brookesia superciliaris* Kuhl. *Sitzungsberichte der Mathematisch-Naturwissenschaftlichen Classe der Kaiserlichen Akademie der Wissenschaften*, *102*, 71–118.

Spinner, M., Westhoff, G., & Gorb, S. N. (2013). Subdigital and subcaudal microornamentation in Chamaeleonidae—A comparative study. *Journal of Morphology*, *274*, 713–723.

Stanley, E. L. (2013). *Systematics and morphological diversification of the Cordylidae (Squamata)*. New York, NY: Dissertation, Richard Gilder Graduate School at the American Museum of Natural History.

Strahm, M. H., & Schwartz, A. (1977). Osteoderms in the anguid lizard subfamily Diploglossinae and their taxonomic importance. *Biotropica*, *9*, 58–72.

Stuart-Fox, D., & Moussalli, A. (2008). Selection for social signalling drives the evolution of chameleon colour change. *PLoS Biology*, *6*, e25.

Teyssier, J., Saenko, S. V., Van Der Marel, D., & Milinkovitch, M. C. (2015). Photonic crystals cause active colour change in chameleons. *Nature Communications*, *6*, 6368.

Tolley, K. A., Townsend, T. M., & Vences, M. (2013). Large-scale phylogeny of chameleons suggests African origins and Eocene diversification. *Proceedings of the Royal Society B: Biological Sciences*, *280*(1759), 20130184.

Townsend, T., & Larson, A. (2002). Molecular phylogenetics and mitochondrial genomic evolution in the Chamaeleonidae (Reptilia, Squamata). *Molecular Phylogenetics and Evolution*, *23*, 22–36.

Townsend, T. M., Vieites, D. R., Glaw, F., & Vences, M. (2009). Testing species-level diversification hypotheses in Madagascar: The case of microendemic *Brookesia* leaf chameleons. *Systematic Biology*, *58*, 641–656.

van der Hoeven, J. (1831). *Icones ad illustrandas coloris mutationes in cha. maeleonte*. Lugduni Batavorum [Leiden]: J. C. Cyfveer.

Vickaryous, M. K., & Hall, B. K. (2008). Development of the dermal skeleton in *Alligator mississippiensis* (Archosauria, Crocodylia) with comments on the homology of osteoderms. *Journal of Morphology*, *269*, 398–422.

Vickaryous, M. K., Meldrum, G., & Russell, A. P. (2015). Armored geckos: A histological investigation of osteoderm development in *Tarentola* (Phyllodactylidae) and *Gekko* (Gekkonidae) with comments on their regeneration and inferred function. *Journal of Morphology*, *276*, 1345–1357.

Vickaryous, M. K., & Sire, J. Y. (2009). The integumentary skeleton of tetrapods: Origin, evolution, and development. *Journal of Anatomy*, *214*, 441–464.

Wiegman, A. F. (1828). Beyträge zur Amphibienkunde. *Isis von Oken*, *21*, 364–383.

Yushkevich, P. A., Piven, J., Hazlett, H. C., Smith, R. G., Ho, S., Gee, J. C., & Gerig, G. (2006). User-guided 3D active contour segmentation of anatomical structures: Significantly improved efficiency and reliability. *NeuroImage*, *31*, 1116–1128.

Zylberberg, L., & Castanet, J. (1985). New data on the structure and the growth of the osteoderms in the reptile *Anguis fragilis* L. (Anguidae, Squamata). *Journal of Morphology*, *186*, 327–342.

SUPPORTING INFORMATION

Additional supporting information may be found online in the Supporting Information section at the end of this article.

How to cite this article: Schucht PJ, Rühr PT, Geier B, Glaw F, Lambertz M. Armored with skin and bone: A combined histological and μCT-study of the exceptional integument of the Antsingy leaf chameleon *Brookesia perarmata* (Angel, 1933). *Journal of Morphology*. 2020;1–11. https://doi.org/10.1002/jmor.21135